

Supporting Information

A novel synergistic confinement strategy for controlled synthesis of high-entropy alloys electrocatalysts

Huining Li,^a Han Zhu,^{a,*} Qikai Shen,^b Shaoda Huang,^a Shuanglong Lu,^a Piming Ma,^a Weifu Dong,^a Mingliang Du^{a,*}

^aKey Laboratory of Synthetic and Biological Colloids, Ministry of Education, School of Chemical and Material Engineering, Jiangnan University, Wuxi 214122, P. R. China

^bCAS Key Laboratory of Molecular Nanostructure and Nanotechnology Institute of Chemistry, Chinese Academy of Sciences, Beijing 100190, China

**Corresponding authors E-mail: zhysw@jiangnan.edu.cn; du@jiangnan.edu.cn*

Table of Contents

1. Materials and Methods	S2
2. Characterizations	S4
3. Electrochemical measurements	S4
4. Supporting Figures (Figs. S1-S15)	S7
References	S13

1. Materials and Methods

Chemicals: Dopamine hydrochloride (99%), Tris(hydroxymethyl)-aminomethane (99%), 1,10-phenanthroline (anhydrous, 99%) and palladium (II) acetate were provided from Alfa Aesar. Urea (AR) was provided from Shanghai Chemical Reagents, China. Cobalt (II) acetate tetrahydrate ($\text{Co}(\text{OAc})_2 \cdot 4\text{H}_2\text{O}$), nickel (II) acetate tetrahydrate ($\text{Ni}(\text{OAc})_2 \cdot 4\text{H}_2\text{O}$), cupric acetate monohydrate ($\text{Cu}(\text{OAc})_2 \cdot \text{H}_2\text{O}$), manganese (II) acetate tetrahydrate ($\text{Mn}(\text{OAc})_2 \cdot 4\text{H}_2\text{O}$) and zinc acetate dihydrate ($\text{Zn}(\text{OAc})_2 \cdot 2\text{H}_2\text{O}$) were obtained from Sinpharm Chemical Reagent Co., Ltd.

Preparation of mpg- C_3N_4 nanosheets: mpg- C_3N_4 nanosheets were produced according to a procedure described in a previous paper.^[1] In a typical experiment, 10 g of urea was placed in a crucible with a cover, and then it was heated at 550 °C within 4 hours in a muffle furnace and then kept for another 4 hours. The resultant yellow powder was collected for use without further treatment.

Preparation of FeCoNiCuPd HEA-NPs: Ferrous acetate (22 mg, 0.12 mmol), cobalt (II) acetate tetrahydrate (30 mg, 0.12 mmol), nickel (II) acetate tetrahydrate (55 mg, 0.22 mmol), cupric acetate monohydrate (24 mg, 0.12 mmol), palladium (II) acetate (27 mg, 0.12 mmol) and 1,10-phenanthroline (357 mg, 1.98 mmol) (Co : phenanthroline = 1:2 molar ratio, Fe/Ni/Cu/Pd : phenanthroline = 1:3 molar ratio) were stirred in methanol (90 mL) for approximately 15 minutes at room temperature. Then, 1 g mpg- C_3N_4 was added and the whole reaction mixture was refluxed at 80 °C for 4 hours. The reaction mixture was cooled to room temperature. Then, prepared Tris methanol solution (1.2 g, 80 mL) was added in the above reaction mixture quickly and stirred for 5 minutes. After that, DA methanol solution (1.2 g, 30 mL) was added quickly. After stirring for 24 hours, the precipitates were collected by centrifugation and washed with ethanol for three times and dried at 60 °C for 12 h. The powder of $\text{M}(\text{phen})_x/\text{mpg-}\text{C}_3\text{N}_4@\text{PDA}$ was transferred into a rectangle crucible placed in a tube furnace and then heated to 1000 °C for 30 min at the heating rate of 5 °C/min under flowing Ar gas and then cooled down at rate of 30 °C/min. When

cooled to room temperature the FeCoNiCuPd HEA-NPs was obtained. The total metal content was 9.53 wt% according to the ICP-AES. The FeCoNiCu and FeCoNi alloy nanoparticles were synthesized using a similar synthetic route, without the addition of palladium (II) acetate, palladium (II) acetate and cupric acetate monohydrate, respectively. The FeCoNiCuMn and FeCoNiMnPd HEA-NPs were synthesized using a similar synthetic route, except for the change of metal salts. Their total metal contents were 4.93 wt% and 5.36 wt% according to the ICP-AES, respectively.

Preparation of FeCoNiCuPd-no phen and FeCoNiCuPd-GO: FeCoNiCuPd-no phen was synthesized using a similar synthetic route, without the addition of 1,10-phenanthroline. FeCoNiCuPd-GO was synthesized using a similar synthetic route, except for the use of graphene oxide instead of mpg-C₃N₄.

Preparation of FeCoNiCuPd-RF: Ferrous acetate (22 mg, 0.12 mmol), cobalt (II) acetate tetrahydrate (30 mg, 0.12 mmol), nickel (II) acetate tetrahydrate (55 mg, 0.22 mmol), cupric acetate monohydrate (24 mg, 0.12 mmol), palladium (II) acetate (27 mg, 0.12 mmol) and 1,10-phenanthroline (357 mg, 1.98 mmol) (Co : phenanthroline = 1:2 molar ratio, Fe/Ni/Cu/Pd : phenanthroline = 1:3 molar ratio) were stirred in water (60 mL) for approximately 15 minutes at room temperature. Then, 1 g mpg-C₃N₄ was added and the whole reaction mixture was refluxed at 80 °C for 4 hours. The reaction mixture was cooled to room temperature. Then, prepared NH₃·H₂O solution (250 μL 28 wt% NH₃·H₂O, 45 mL water) was added in the above reaction mixture quickly and stirred for 5 minutes. After that, 500 mg resorcinol and formaldehyde solution (700 μL 37 wt% formaldehyde, 45 mL water) was added quickly. After stirring for 24 hours at room temperature, the precipitates were collected by centrifugation and washed with water and ethanol for four times and dried at 60 °C for 12 h. The powder of M(phen)_x/mpg-C₃N₄@RF was transferred into a rectangle crucible placed in a tube furnace and then heated to 1000 °C for 30 min at the heating rate of 5 °C/min under flowing Ar gas and then cooled down at rate of 30 °C/min.

2. Characterizations

Powder X-ray diffraction patterns were recorded on a Rigaku D/max2500 with Cu K α radiation (40kV, 40mA, 0.1541nm). The metal content of the samples was analyzed by inductively coupled plasma optical emission spectroscopy (ICP-OES) using an Agilent 720ES spectrometer. The surface morphology and the element distribution of the samples were obtained using a transmission electron microscope (TEM, JEOL, JEM-2100F) with energy-dispersive X-ray spectroscopy (EDS) analysis. High-angle annular dark-field scanning TEM (HAADF-STEM) and high resolution transmission electron microscopy (HRTEM) were conducted by a Tecnai G2 F30S-Twin equipment at an accelerating voltage of 300 kV. X-ray photoelectron spectroscopy (XPS, Kratos Axis supra) analyses were acquired with an aluminum (mono) K α source (1486.6 eV). Thermo gravimetric analyses (TGA) were carried out on a TA-60 WS thermal analyser heating from room temperature to 1000 °C at the rate of 2 °C/min under flowing nitrogen.

3. Electrochemical measurements

ORR: The FeCoNiCuPd HEA-NPs, FeCoNiCu, FeCoNi alloy nanoparticles and 20wt% Pt/C samples were prepared by ultrasonically mixing 3.0 mg of the catalyst powder with the mixture of 400 μ L isopropanol, 100 μ L H₂O and 50 μ L 5% Nafion solution for 60 min to form homogeneous catalyst inks. Next, 10 μ L catalyst ink was carefully dropped onto the polished glassy carbon rotating disk electrode (RDE) or rotating ring disk electrode (RRDE).

The ORR measurements were performed by using a glassy carbon rotating disk electrode (RDE; diameter, 5 mm; area, 0.196 cm²) and rotating ring-disk electrode (RRDE; disk diameter, 5.61 mm; area, 0.247 cm²) setup (Pine, USA). A saturated calomel electrode (SCE) was used as the reference electrode, and a carbon rod (diameter, 3 mm; area, 0.0761 cm²) was used as the counter electrode. The electrolyte was 0.1 M KOH solution. The potential scan rate was 50 mV s⁻¹ for the CV

measurements in N₂-purged 0.1 M KOH electrolyte, and the potential was scanned from 0.01 to 1.26 V versus reversible hydrogen electrode (RHE). The ORR measurement was performed in the O₂-saturated 0.1 M KOH solution (scan rate: 10 mV s⁻¹, rotation speed: varying from 400 to 2025 rpm). The accelerated durability tests (ADT) for all catalysts were conducted in 0.1 M KOH solution by applying the cyclic potential sweeps from 0.6 to 1.0 V versus RHE at a sweep rate of 150 mV s⁻¹ for 3,000 cycles.

All the potentials are mentioned with respected to RHE, which convert from the SCE using $E(\text{RHE}) = E(\text{SCE}) + 0.244 + 0.0591\text{pH}$. The electron transfer number (n) and kinetic current density (J_k) can be calculated from Koutecky-Levich equation: [2]

$$\frac{1}{J} = \frac{1}{J_L} + \frac{1}{J_K} = \frac{1}{B\omega^{\frac{1}{2}}} + \frac{1}{J_K}$$

$$B = 0.2nFC_0D^{\frac{2}{3}}\gamma^{-\frac{1}{6}}$$

where J is the measured current density, J_L and J_K are the limiting and kinetic current densities, ω is the rotation speed of the electrode (rpm), n is the electron transfer number, F is the Faraday constant (96485 C mol⁻¹), C_0 is the bulk concentration of O₂ in 0.1 M KOH solution (1.2×10^{-6} mol cm⁻³), D is the diffusion coefficient of O₂ (1.9×10^{-5} cm² s⁻¹) in 0.1 M KOH solution, and γ is the kinematic viscosity of the electrolyte (0.01 cm² s⁻¹).

For the RRDE measurements, the n and hydrogen peroxide selectivity (H₂O₂%) can be determined by the following equation:

$$n = \frac{4I_D}{I_D + \frac{I_R}{N}}$$

$$H_2O_2(\%) = \frac{200I_R}{I_D N + I_R}$$

where I_D is the disk current, I_R is the ring current, and $N=0.37$ is the current collection efficiency of the Pt ring.

OER: An electrochemical workstation (CHI660E, Shanghai Chenhua) was used to obtain the electrochemical measurements in 1.0 M KOH solution. All the electrochemical performance tests were performed with a standard three-electrode system, using the as fabricated catalyst as the working electrode, a graphite rod as the counter electrode, and a saturated calomel electrode (SCE) as the reference electrode. All potentials were referred to the RHE by the following calculations: $E(\text{RHE}) = E(\text{SCE}) + 0.059\text{pH} + 0.244$. 3.0 mg of the catalyst powder with the mixture of 400 μL isopropanol, 100 μL H_2O and 50 μL 5% Nafion solution for 60 min to form homogeneous catalyst inks. Next, 5 μL catalyst ink was carefully dropped onto the polished glassy carbon electrode of 3 mm in diameter. Linear sweep voltammetry with a scan rate of 5 mV/s was conducted in 1 M KOH. Electrochemical impedance spectroscopy (EIS) was tested at open circuit voltage from 0.01 Hz to 100 kHz with an amplitude of 5 mV.

4. Supporting Figures (Figs. S1-S14)

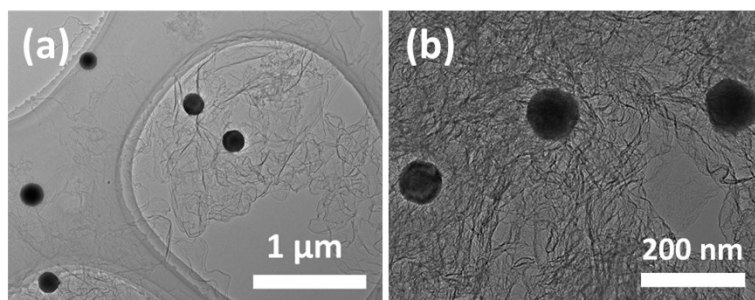


Fig. S1. Representative TEM images of the obtained FeCoNiCuPd HEA-NPs prepared with mpg-C₃N₄ as matrix at different magnifications.

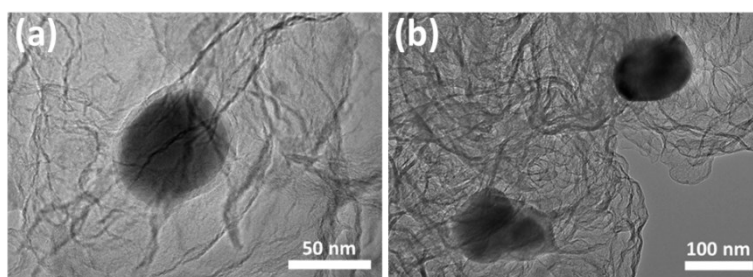


Fig. S2. Representative TEM images of the (a) FeCoNi and (b) FeCoNiCu alloys prepared with mpg-C₃N₄ as matrix.

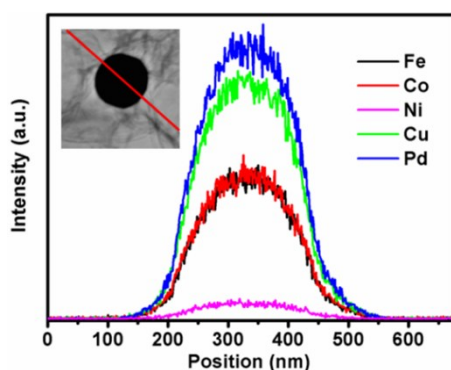


Fig. S3. EDS line scanning images of the FeCoNiCuPd homogeneous HEA-NPs.

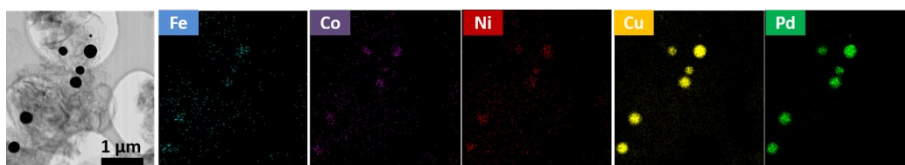


Fig. S4. EDS maps for FeCoNiCuPd-RF at low magnifications.

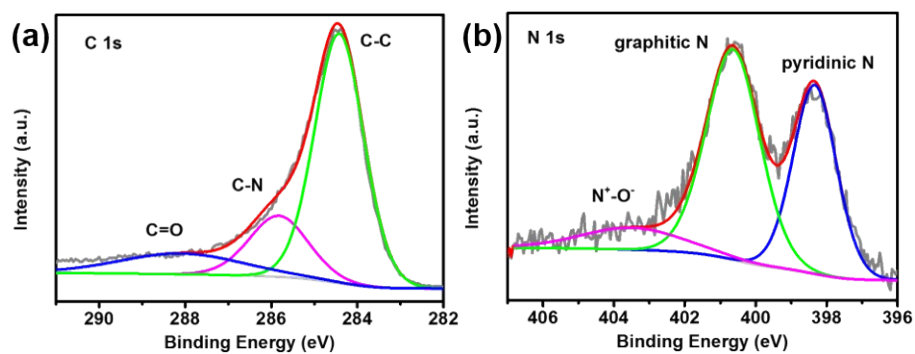


Fig. S5. XPS spectra of (a) C 1s and (b) N 1s of FeCoNiCuPd HEA-NPs.

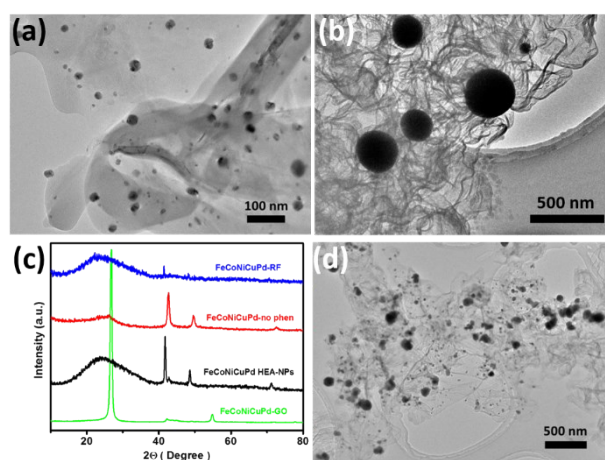


Fig. S6. TEM images of (a) FeCoNiCuPd-GO and (b) FeCoNiCuPd-RF. (c) XRD patterns of FeCoNiCuPd HEA-NPs, FeCoNiCuPd-GO, FeCoNiCuPd-RF, and FeCoNiCuPd-no phen. (d) TEM images of FeCoNiCuPd-phen.

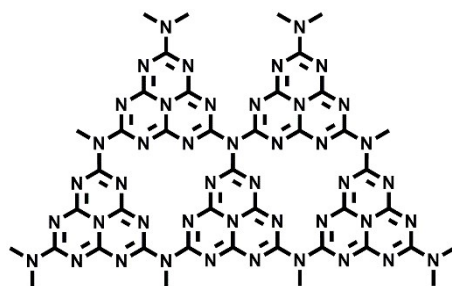


Fig. S7. Schematic illustration of the structure of mpg-C₃N₄.

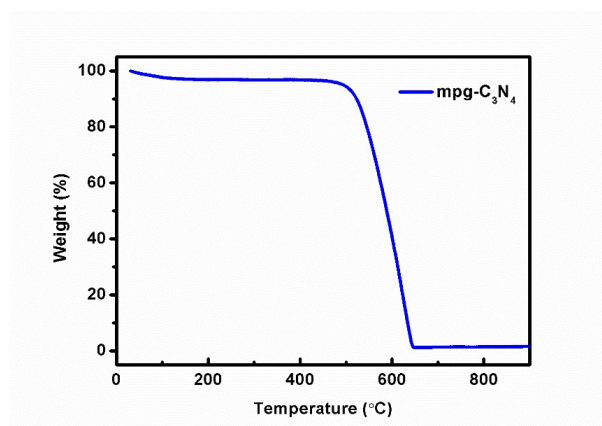


Fig. S8. TGA curve of g-C₃N₄ nanosheets.

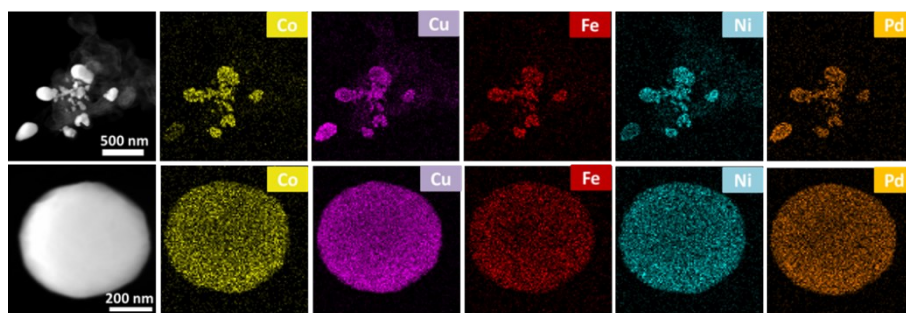


Fig. S9. EDS maps for FeCoNiCuPd-no phen at different magnifications.

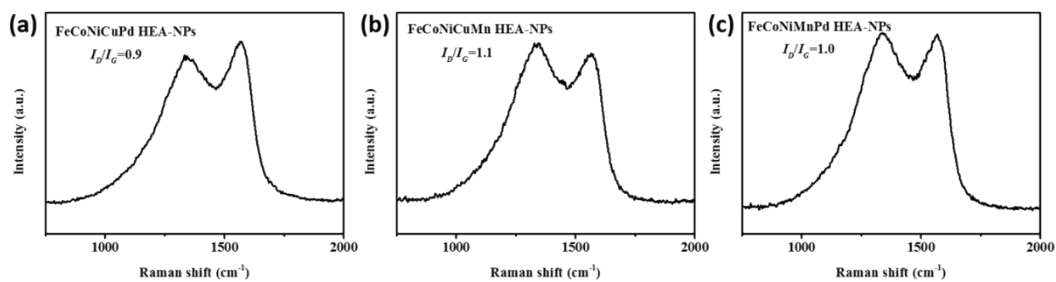


Fig. S10. The Raman spectra of the N-doped carbon of (a) FeCoNiCuPd, (b) FeCoNiCuMn and (c) FeCoNiMnPd HEA-NPs.

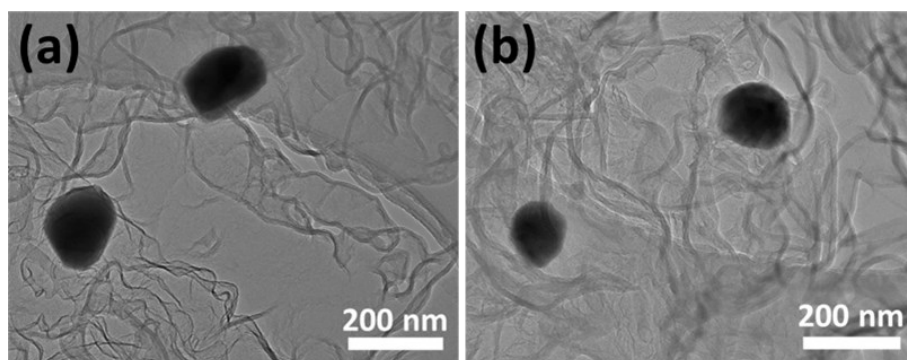


Fig. S11. TEM images of (a) FeCoNiMnPd and (b) FeCoNiCuMn HEA-NPs.

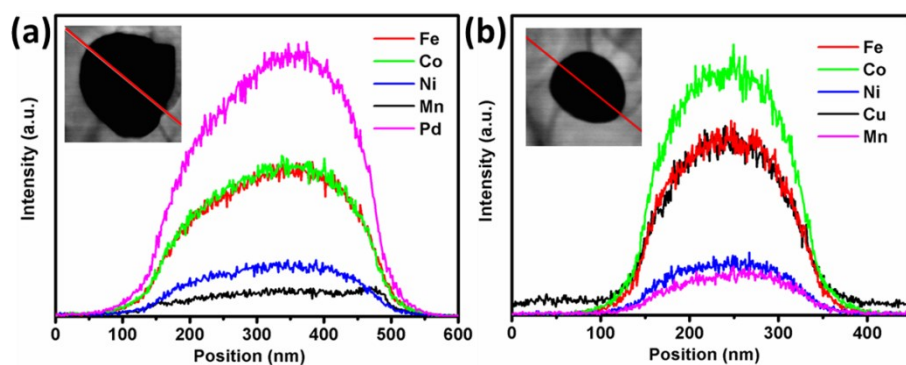


Fig. S12. EDS line scanning images of (a) FeCoNiMnPd and (b) FeCoNiCuMn HEA-NPs.

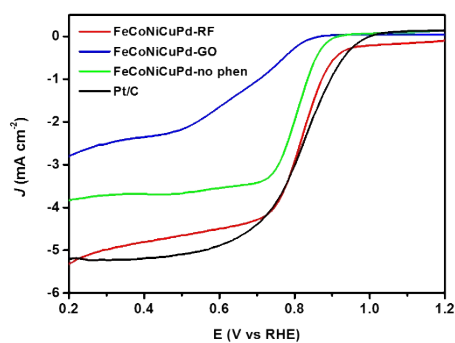


Fig. S13. ORR polarization plots of FeCoNiCuPd-no phen, FeCoNiCuPd-GO, FeCoNiCuPd-RF and commercial Pt/C recorded in O₂-saturated 0.1 M NaOH solution at a scan rate of 10 mV s⁻¹ and a rotation rate of 1600 rpm.

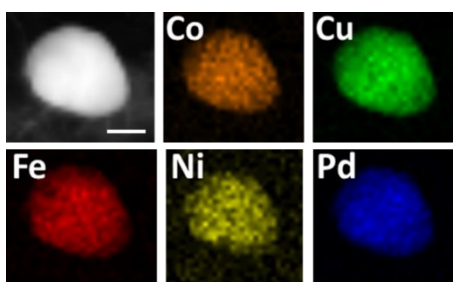


Fig. S14. HAADF-STEM and EDS mapping images of the FeCoNiCuPd HEA-NPs after ORR cycles, the scale bar is 100 nm.

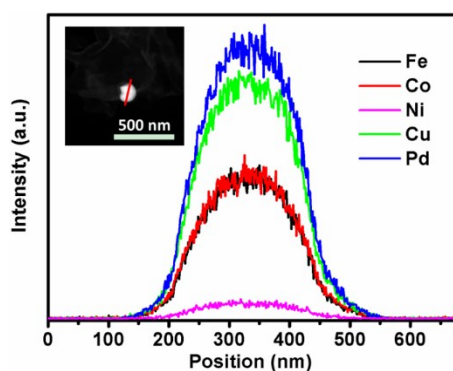


Fig. S15. HAADF-STEM and EDS line scanning image of the FeCoNiCuPd HEA-NPs after ORR cycles.

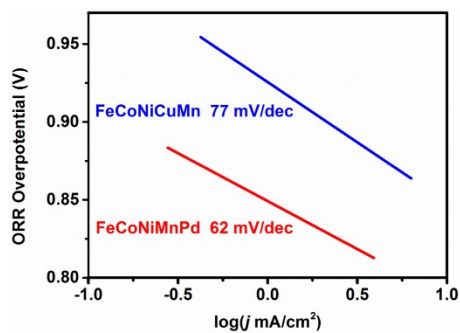


Fig. S16. ORR Tafel plots derived from the LSV curves of FeCoNiCuMn and FeCoNiMnPd.

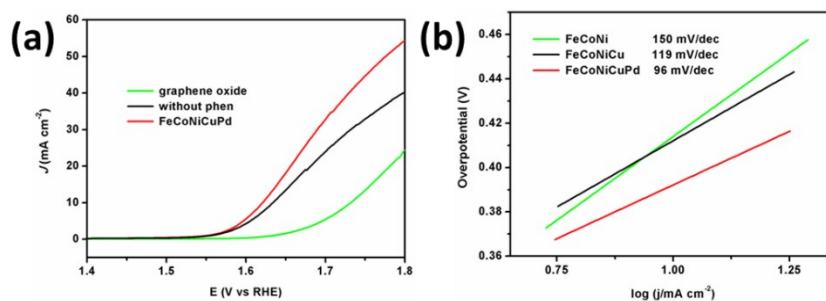


Fig. S17. (a) OER polarizations of FeCoNiCuPd HEA-NPs, FeCoNiCuPd-no phen and FeCoNiCuPd-GO. (b) Tafel curves of FeCoNiCuPd HEA-NPs, FeCoNi and FeCoNiCu alloys.

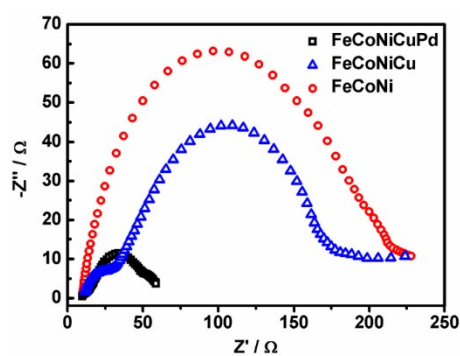


Fig. S18. The electrochemical impedance spectroscopy of FeCoNiCuPd HEA-NPs,

References

- [1] Y. Feng, Q. Shao, Y. Ji, X. Cui, Y. Li, X. Zhu, X. Huang, *Sci. Adv.* **2018**, *4*, eaap8817.
- [2] J. Liu, Y. Yu, R. Qi, C. Cao, X. Liu, Y. Zheng, W. Song, *Appl. Catal. B, Environ.* **2019**, *244*, 459.